

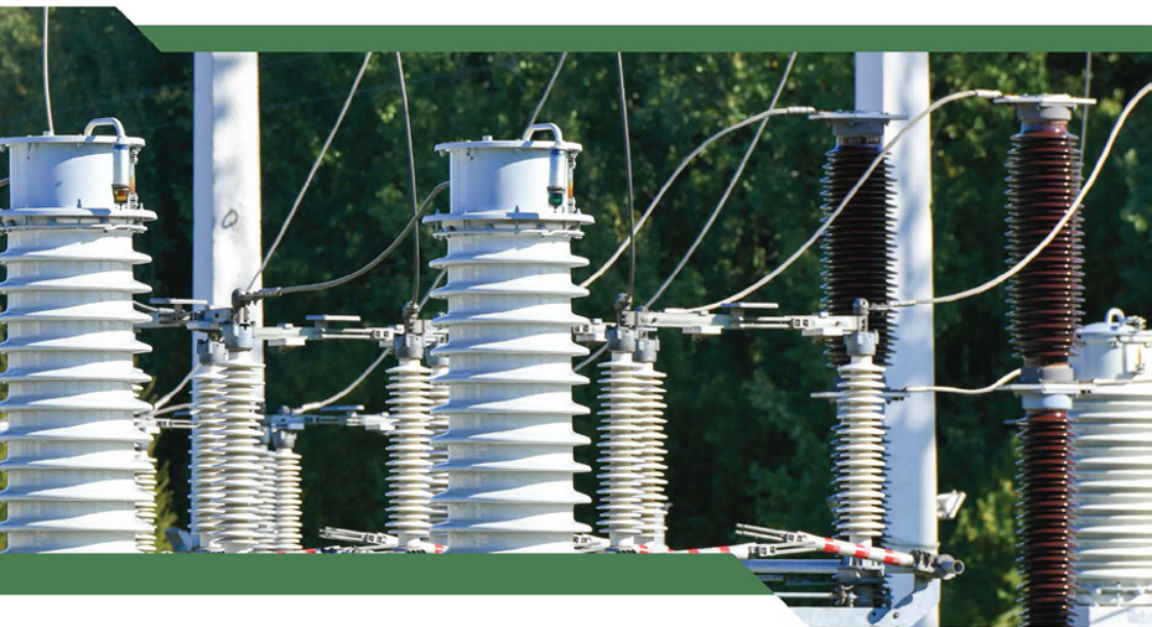


IEEE Press Series on Power and Energy Systems
Ganesh Kumar Venayagamoorthy, Series Editor

Modular Multilevel Converters

Control, Fault Detection, and Protection

Fujin Deng, Chengkai Liu, Zhe Chen




IEEE PRESS

WILEY

Modular Multilevel Converters

IEEE Press
445 Hoes Lane
Piscataway, NJ 08854

IEEE Press Editorial Board
Sarah Spurgeon, *Editor in Chief*

Jón Atli Benediktsson
Anjan Bose
James Duncan
Amin Moeness
Desineni Subbaram Naidu

Behzad Razavi
Jim Lyke
Hai Li
Brian Johnson

Jeffrey Reed
Diomidis Spinellis
Adam Drobot
Tom Robertazzi
Ahmet Murat Tekalp

Modular Multilevel Converters

Control, Fault Detection, and Protection

Fujin Deng
Southeast University
Nanjing, China

Chengkai Liu
Southeast University
Nanjing, China

Zhe Chen
Aalborg University
Aalborg, Denmark



IEEE Press Series on Power and Energy Systems
Ganesh Kumar Venayagamoorthy, Series Editor


IEEE PRESS
WILEY

Copyright © 2023 by The Institute of Electrical and Electronics Engineers, Inc.
All rights reserved.

Published by John Wiley & Sons, Inc., Hoboken, New Jersey.
Published simultaneously in Canada.

No part of this publication may be reproduced, stored in a retrieval system, or transmitted in any form or by any means, electronic, mechanical, photocopying, recording, scanning, or otherwise, except as permitted under Section 107 or 108 of the 1976 United States Copyright Act, without either the prior written permission of the Publisher, or authorization through payment of the appropriate per-copy fee to the Copyright Clearance Center, Inc., 222 Rosewood Drive, Danvers, MA 01923, (978) 750-8400, fax (978) 750-4470, or on the web at www.copyright.com. Requests to the Publisher for permission should be addressed to the Permissions Department, John Wiley & Sons, Inc., 111 River Street, Hoboken, NJ 07030, (201) 748-6011, fax (201) 748-6008, or online at <http://www.wiley.com/go/permission>.

Trademarks: Wiley and the Wiley logo are trademarks or registered trademarks of John Wiley & Sons, Inc. and/or its affiliates in the United States and other countries and may not be used without written permission. All other trademarks are the property of their respective owners. John Wiley & Sons, Inc. is not associated with any product or vendor mentioned in this book.

Limit of Liability/Disclaimer of Warranty: While the publisher and author have used their best efforts in preparing this book, they make no representations or warranties with respect to the accuracy or completeness of the contents of this book and specifically disclaim any implied warranties of merchantability or fitness for a particular purpose. No warranty may be created or extended by sales representatives or written sales materials. The advice and strategies contained herein may not be suitable for your situation. You should consult with a professional where appropriate. Neither the publisher nor author shall be liable for any loss of profit or any other commercial damages, including but not limited to special, incidental, consequential, or other damages. Further, readers should be aware that websites listed in this work may have changed or disappeared between when this work was written and when it is read. Neither the publisher nor authors shall be liable for any loss of profit or any other commercial damages, including but not limited to special, incidental, consequential, or other damages.

For general information on our other products and services or for technical support, please contact our Customer Care Department within the United States at (800) 762-2974, outside the United States at (317) 572-3993 or fax (317) 572-4002.

Wiley also publishes its books in a variety of electronic formats. Some content that appears in print may not be available in electronic formats. For more information about Wiley products, visit our website at www.wiley.com.

Library of Congress Cataloging-in-Publication Data

Names: Deng, Fujin, author. | Liu, Chengkai, author. | Chen, Zhe, author.

Title: Modular multilevel converters : control, fault detection, and protection / Fujin Deng, South East University, Nanjing, China, Chengkai Liu, South East University, Nanjing, China, Zhe Chen, Aalborg University, Aalborg, DA, Denmark.

Description: Hoboken, New Jersey : Wiley-IEEE Press, [2023] | Series: IEEE Press series on power and energy systems | Includes bibliographical references and index.

Identifiers: LCCN 2022052863 (print) | LCCN 2022052864 (ebook) | ISBN 9781119875604 (cloth) | ISBN 9781119875611 (adobe pdf) | ISBN 9781119875628 (epub)

Subjects: LCSH: Electric current converters. | Modularity (Engineering)

Classification: LCC TK7872.C8 D455 2023 (print) | LCC TK7872.C8 (ebook) | DDC 621.3815/322-dc23/eng/20230103

LC record available at <https://lccn.loc.gov/2022052863>

LC ebook record available at <https://lccn.loc.gov/2022052864>

Cover Design: Wiley

Cover Images: © KAY4YK/Shutterstock

Set in 9.5/12.5pt STIXTwoText by Straive, Pondicherry, India

Contents

About the Authors *xiii*

Preface *xv*

| | | |
|----------|--------------------------------------|----------|
| 1 | Modular Multilevel Converters | 1 |
| 1.1 | Introduction | 1 |
| 1.2 | MMC Configuration | 2 |
| 1.2.1 | Converter Configuration | 2 |
| 1.2.2 | Submodule Configuration | 2 |
| 1.3 | Operation Principles | 3 |
| 1.3.1 | Submodule Normal Operation | 3 |
| 1.3.2 | Submodule Blocking Operation | 5 |
| 1.3.3 | Converter Operation | 6 |
| 1.4 | Modulation Scheme | 8 |
| 1.4.1 | Phase-Disposition PWM | 9 |
| 1.4.2 | Phase-Shifted PWM | 10 |
| 1.4.3 | Nearest Level Modulation | 11 |
| 1.5 | Mathematical Model | 12 |
| 1.5.1 | Submodule Mathematical Model | 12 |
| 1.5.1.1 | Switching-Function Based Model | 13 |
| 1.5.1.2 | Reference-Based Model | 13 |
| 1.5.2 | Arm Mathematical Model | 14 |
| 1.5.2.1 | Switching-Function Based Model | 14 |
| 1.5.2.2 | Reference-Based Model | 15 |
| 1.5.3 | Three-Phase MMC Mathematical Model | 16 |
| 1.5.3.1 | AC-Side Mathematical Model | 17 |
| 1.5.3.2 | DC-Side Mathematical Model | 17 |
| 1.6 | Design Constraints | 18 |
| 1.6.1 | Power Device Design | 18 |

| | | |
|----------|--|-----------|
| 1.6.1.1 | Rated Voltage of Power Devices | 19 |
| 1.6.1.2 | Rated Current of Power Devices | 19 |
| 1.6.2 | Capacitor Design | 21 |
| 1.6.3 | Arm Inductor Design | 23 |
| 1.7 | Faults Overview of MMCs | 24 |
| 1.7.1 | Internal Faults of MMCs | 24 |
| 1.7.2 | External Faults of MMCs | 25 |
| 1.8 | Summary | 25 |
| | References | 26 |
| 2 | Control of MMCs | 29 |
| 2.1 | Introduction | 29 |
| 2.2 | Overall Control of MMCs | 30 |
| 2.3 | Output Control of MMCs | 31 |
| 2.3.1 | Current Control | 31 |
| 2.3.2 | Power and DC-Link Voltage Control | 33 |
| 2.3.3 | Grid Forming Control | 36 |
| 2.4 | Centralized Capacitor Voltage Balancing Control | 38 |
| 2.4.1 | On-State SMs Number Based VBC | 39 |
| 2.4.2 | Balancing Adjusting Number Based VBC | 39 |
| 2.4.2.1 | Capacitor VBC | 40 |
| 2.4.2.2 | SM Switching Frequency | 40 |
| 2.4.3 | IPSC-PWM Harmonic Current Based VBC | 42 |
| 2.4.3.1 | IPSC-PWM Scheme | 42 |
| 2.4.3.2 | High-Frequency Arm Current | 43 |
| 2.4.3.3 | Arm Capacitor Voltage Analysis | 46 |
| 2.4.3.4 | Voltage Balancing Control | 47 |
| 2.4.4 | SHE-PWM Pulse Energy Sorting Based VBC | 53 |
| 2.4.4.1 | MMCs Analysis with Grid-Frequency Pulses | 53 |
| 2.4.4.2 | Charge Transfer of Capacitors in Lower Arm | 56 |
| 2.4.4.3 | Charge Transfer of Capacitors in Upper Arm | 57 |
| 2.4.4.4 | Voltage Balancing Control | 59 |
| 2.4.5 | PSC-PWM Pulse Energy Sorting Based VBC | 65 |
| 2.4.5.1 | MMC with PSC-PWM | 65 |
| 2.4.5.2 | Capacitor Charge Transfer Under Linearization Method | 67 |
| 2.4.5.3 | Capacitor Voltage Analysis | 70 |
| 2.4.5.4 | Voltage Balancing Control | 72 |
| 2.5 | Individual Capacitor Voltage Balancing Control | 79 |
| 2.5.1 | Average and Balancing Control Based VBC | 79 |
| 2.5.1.1 | Average Control | 80 |
| 2.5.1.2 | Balancing Control | 80 |

| | | |
|----------|--|------------|
| 2.5.2 | Reference Modulation Index Based VBC | 81 |
| 2.5.2.1 | Analysis of Capacitor Voltage | 82 |
| 2.5.2.2 | Control of i_{cdc} by Modulation Index m | 83 |
| 2.5.2.3 | Voltage Balancing Control by m | 84 |
| 2.5.3 | Reference Phase Angle Based VBC | 86 |
| 2.5.3.1 | Control of i_{cdc} by Phase Angle θ | 86 |
| 2.5.3.2 | Voltage Balancing Control by θ | 87 |
| 2.6 | Circulating Current Control | 94 |
| 2.6.1 | Proportional Integration Control | 95 |
| 2.6.2 | Multiple Proportional Resonant Control | 97 |
| 2.6.3 | Repetitive Control | 98 |
| 2.7 | Summary | 100 |
| | References | 100 |
| 3 | Fault Detection of MMCs under IGBT Faults | 103 |
| 3.1 | Introduction | 103 |
| 3.2 | IGBT Faults | 104 |
| 3.2.1 | IGBT Short-Circuit Fault | 105 |
| 3.2.2 | IGBT Open-Circuit Fault | 105 |
| 3.3 | Protection and Detection Under IGBT Short-Circuit Faults | 106 |
| 3.3.1 | SM Under IGBT Short-Circuit Fault | 106 |
| 3.3.2 | Protection and Detection Under IGBT Short-Circuit Fault | 107 |
| 3.4 | MMC Features Under IGBT Open-Circuit Faults | 109 |
| 3.4.1 | Faulty SM Features Under T_1 Open-Circuit Fault | 109 |
| 3.4.2 | Faulty SM Features Under T_2 Open-Circuit Fault | 110 |
| 3.4.2.1 | Operation Mode of Faulty SM | 110 |
| 3.4.2.2 | Faulty SM Capacitor Voltage of MMCs in Inverter Mode | 111 |
| 3.4.2.3 | Faulty SM Capacitor Voltage of MMCs in Rectifier Mode | 112 |
| 3.5 | Kalman Filter Based Fault Detection Under IGBT Open-Circuit Faults | 115 |
| 3.5.1 | Kalman Filter Algorithm | 117 |
| 3.5.2 | Circulating Current Estimation | 118 |
| 3.5.3 | Faulty Phase Detection | 119 |
| 3.5.4 | Capacitor Voltage | 120 |
| 3.5.5 | Faulty SM Detection | 121 |
| 3.6 | Integrator Based Fault Detection Under IGBT Open-Circuit Faults | 127 |
| 3.7 | STW Based Fault Detection Under IGBT Open-Circuit Faults | 132 |
| 3.7.1 | MMC Data | 132 |
| 3.7.2 | Sliding-Time Windows | 133 |
| 3.7.3 | Feature of STW | 134 |
| 3.7.4 | Features Relationships Between Neighboring STWs | 137 |

- 3.7.5 Features Extraction Algorithm 137
- 3.7.6 Energy Entropy Matrix 138
- 3.7.7 2D-CNN 138
- 3.7.8 Fault Detection Method 140
- 3.7.9 Selection of Sliding Interval 141
- 3.7.10 Analysis of Fault Localization Time 142
- 3.8 IF Based Fault Detection Under IGBT Open-Circuit Faults 145
 - 3.8.1 IT for MMCs 145
 - 3.8.2 SM Depth in IT 146
 - 3.8.3 IF for MMCs 147
 - 3.8.4 SM Average Depth in IF 147
 - 3.8.5 IF Output 147
 - 3.8.6 Fault Detection 149
 - 3.8.7 Selection of m_p 150
 - 3.8.8 Selection of k 151
- 3.9 Summary 156
 - References 156

4 Condition Monitoring and Control of MMCs Under Capacitor Faults 161

- 4.1 Introduction 161
- 4.2 Capacitor Equivalent Circuit in MMCs 162
- 4.3 Capacitor Parameter Characteristics in MMCs 164
 - 4.3.1 Capacitor Current Characteristics 164
 - 4.3.2 Capacitor Impedance Characteristics 167
 - 4.3.3 Capacitor Voltage Characteristics 167
- 4.4 Capacitor Aging 169
- 4.5 Capacitance Monitoring 171
 - 4.5.1 Capacitor Voltage and Current Based Monitoring Strategy 172
 - 4.5.2 Arm Average Capacitance Based Monitoring Method 172
 - 4.5.2.1 Equivalent Arm Structure 172
 - 4.5.2.2 Capacitor Monitoring Method 173
 - 4.5.3 Reference SM based Monitoring Method 179
 - 4.5.3.1 Principle of the RSM-Based Capacitor Monitoring Strategy 179
 - 4.5.3.2 Capacitor Monitoring-Based Voltage-Balancing Control 180
 - 4.5.3.3 Selection of RSM 182
 - 4.5.3.4 Capacitor Monitoring Strategy 183
 - 4.5.4 Sorting-Based Monitoring Strategy 189
 - 4.5.5 Temperature Effect of Capacitance 195
- 4.6 ESR Monitoring 195
 - 4.6.1 Direct ESR Monitoring Strategy 196

| | | |
|-------|---|-----|
| 4.6.2 | Sorting-Based ESR Monitoring Strategy | 196 |
| 4.6.3 | Temperature Effect of ESR | 203 |
| 4.7 | Capacitor Lifetime Monitoring | 204 |
| 4.8 | Arm Current Optimal Control Under Capacitor Aging | 205 |
| 4.8.1 | Equivalent Circuit of MMCs | 205 |
| 4.8.2 | Arm Current Characteristics | 207 |
| 4.8.3 | Arm Current Optimal Control | 208 |
| 4.9 | SM Power Losses Optimal Control Under Capacitor Aging | 212 |
| 4.9.1 | Equivalent SM Reference | 213 |
| 4.9.2 | SM Conduction Losses | 215 |
| 4.9.3 | SM Switching Losses | 216 |
| 4.9.4 | SM Power Losses Optimal Control | 217 |
| 4.10 | Summary | 225 |
| | References | 226 |

5 Fault-Tolerant Control of MMCs Under SM Faults 229

| | | |
|-------|--|-----|
| 5.1 | Introduction | 229 |
| 5.2 | SM Protection Circuit | 229 |
| 5.3 | Redundant Submodules | 230 |
| 5.4 | Fault-Tolerant Scheme | 231 |
| 5.4.1 | Cold Reserve Mode | 232 |
| 5.4.2 | Spinning Reserve Mode-I | 233 |
| 5.4.3 | Spinning Reserve Mode-II | 235 |
| 5.4.4 | Spinning Reserve Mode-III | 235 |
| 5.4.5 | Comparison of Fault-Tolerant Schemes | 235 |
| 5.5 | Fundamental Circulating Current Elimination Based Tolerant Control | 236 |
| 5.5.1 | Equivalent Circuit of MMCs | 236 |
| 5.5.2 | Fundamental Circulating Current | 238 |
| 5.5.3 | Fundamental Circulating Current Elimination Control | 239 |
| 5.5.4 | Control Analysis | 241 |
| 5.6 | Summary | 247 |
| | References | 247 |

6 Control of MMCs Under AC Grid Faults 249

| | | |
|---------|---|-----|
| 6.1 | Introduction | 249 |
| 6.2 | Mathematical Model of MMCs under AC Grid Faults | 250 |
| 6.2.1 | AC-Side Mathematical Model | 250 |
| 6.2.1.1 | MMC with AC-Side Transformer | 250 |
| 6.2.1.2 | MMCs without AC-Side Transformer | 252 |
| 6.2.2 | Instantaneous Power Mathematical Model | 253 |

| | | |
|---------|--|-----|
| 6.3 | AC-Side Current Control of MMCs under AC Grid Faults | 254 |
| 6.3.1 | Positive- and Negative-Sequence Current Control | 255 |
| 6.3.1.1 | Inner Loop Current Control | 255 |
| 6.3.1.2 | Outer Power Control | 256 |
| 6.3.2 | Zero-Sequence Current Control | 257 |
| 6.3.3 | Proportional Resonant Based Current Control | 259 |
| 6.4 | Circulating Current Suppression Control of MMCs under AC Grid Faults | 261 |
| 6.4.1 | Circulating Current of MMCs Under AC Grid Faults | 261 |
| 6.4.2 | Single-Phase Vector Based Control | 262 |
| 6.4.3 | $\alpha\beta 0$ Stationary Frame Based Control | 264 |
| 6.4.4 | Three-Phase Stationary Frame Based Control | 266 |
| 6.4.4.1 | Positive- and Negative-Sequence Controller | 267 |
| 6.4.4.2 | Zero-Sequence Controller | 268 |
| 6.5 | Summary | 269 |
| | References | 270 |

7 Protection Under DC Short-Circuit Fault in HVDC System 273

| | | |
|---------|---|-----|
| 7.1 | Introduction | 273 |
| 7.2 | MMC Under DC Short-Circuit Fault | 274 |
| 7.2.1 | System Configuration | 274 |
| 7.2.2 | AC Circuit Breaker | 274 |
| 7.2.3 | Protection Thyristor | 275 |
| 7.2.4 | Protection Operation | 276 |
| 7.3 | DC Circuit Breaker Based Protection | 281 |
| 7.3.1 | Mechanical Circuit Breaker | 282 |
| 7.3.2 | Semiconductor Circuit Breaker | 283 |
| 7.3.2.1 | Semi-Controlled Semiconductor Circuit Breaker | 283 |
| 7.3.2.2 | Fully Controlled Semiconductor Circuit Breaker | 284 |
| 7.3.3 | Hybrid Circuit Breaker | 285 |
| 7.3.3.1 | Conventional Hybrid Circuit Breaker | 285 |
| 7.3.3.2 | Proactive Hybrid Circuit Breaker | 286 |
| 7.3.4 | Multiterminal Circuit Breaker | 287 |
| 7.3.4.1 | Assembly CB | 287 |
| 7.3.4.2 | Multiport CB | 288 |
| 7.3.5 | Superconducting Fault Current Limiter | 289 |
| 7.3.6 | SFCL-Based Circuit Breaker | 289 |
| 7.3.6.1 | SFCL-Based Hybrid Circuit Breaker | 290 |
| 7.3.6.2 | SFCL-Based Self-Oscillating Circuit Breaker | 291 |
| 7.3.6.3 | SFCL-Based Forced Zero-Crossing Circuit Breaker | 292 |
| 7.4 | Fault Blocking Converter Based Protection | 293 |

| | | |
|---------|--|-----|
| 7.4.1 | FB SM and HB SM Based Hybrid MMC | 294 |
| 7.4.2 | Fault Blocking Control | 296 |
| 7.4.3 | FB SM Ratio | 298 |
| 7.4.4 | Alternative Fault Blocking SMs | 298 |
| 7.5 | Bypass Thyristor MMC Based Protection | 299 |
| 7.5.1 | Bypass Thyristor MMC Configuration | 299 |
| 7.5.2 | SM Control | 302 |
| 7.5.3 | Current Interruption Control | 303 |
| 7.5.3.1 | Three-Phase Rectifier Period | 304 |
| 7.5.3.2 | One-Phase Current Interruption Moment | 304 |
| 7.5.3.3 | Single-Phase Rectifier Period | 305 |
| 7.5.3.4 | Three-Phase Current Interruption Moment | 306 |
| 7.5.4 | Protection Operation | 307 |
| 7.6 | CTB-HMMC Based Protection | 311 |
| 7.6.1 | CTB-HMMC Configuration | 312 |
| 7.6.2 | SM Operation Principle | 313 |
| 7.6.3 | Operation Principle for DC Fault Protection | 314 |
| 7.6.4 | DC-Side Current Interruption Operation | 315 |
| 7.6.5 | Capacitor Voltage Increment | 317 |
| 7.6.6 | AC-Side Current Interruption Operation | 318 |
| 7.6.7 | MMC Comparison | 321 |
| 7.6.7.1 | Comparison with Current Blocking SM Based MMCs | 321 |
| 7.6.7.2 | Comparison with Thyristor Based MMCs | 323 |
| 7.7 | Summary | 328 |
| | References | 329 |

| | |
|--------------|-----|
| Index | 333 |
|--------------|-----|

About the Authors



Fujin Deng received the PhD degree in Energy Technology from the Department of Energy Technology, Aalborg University, Aalborg, Denmark, in 2012. From 2013 to 2015 and from 2015 to 2017, he was a postdoctoral researcher and an assistant professor, respectively, in the Department of Energy Technology, Aalborg University, Aalborg, Denmark. He joined Southeast University in 2017 as a professor in the School of Electrical Engineering, Southeast University, Nanjing, China. He also serves as the Head of the Department of Power Electronics in the School of Electrical Engineering, Southeast University.

Dr. Deng has published more than 110 peer-reviewed journal articles and more than 60 conference papers. And he holds more than 50 issued and pending patents. He is a senior member of the IEEE. His main research interests include modular multilevel converters (MMCs), high-voltage direct current (HVDC) technology, DC/DC solid state transformer, fault diagnosis and tolerant control for power converters, DC grid control, and DFIG/PMSG-based wind turbine/farm modeling and control.



Chengkai Liu received the BEng degree in Electrical Engineering from Chien-Shiung WU College of Southeast University, Nanjing, China, in 2018, where he is currently working toward the PhD degree with the School of Electrical Engineering. He was a guest PhD student in the Department of Energy Technology, Aalborg University, Aalborg, Denmark from 2021 to 2022.

Mr. Liu has published 17 peer-reviewed journal articles and held 6 issued Chinese patents. His main research interests include modular multilevel

converters (MMCs), DC grids, fault detection, and DC fault protection. He has participated in several research programs, and his inventions enhance the reliability of the MMC system and reduce the power losses of the converter.

Mr. Liu received a national scholarship for his graduate studies (PhD) from the Chinese Ministry of Education in 2021 and the National First Prize in the National Undergraduate Electronic Design Contest in 2017. He serves as a reviewer for *IEEE Transactions on Power Electronics*, *IEEE Transactions on Power Delivery*, *IEEE Journal of Emerging and Selected Topics in Power Electronics*, *IEEE Transactions on Circuits and Systems II*, and *CSEE Journal of Power and Energy Systems*.



Zhe Chen received his BEng and MSc degrees in Electrical Engineering (power plants and power system automation) from the Northeast China Institute of Electric Power Engineering, Jilin City, China in 1982 and 1986, respectively; MPhil in Power Electronics, from Staffordshire University, England, in 1993; and the PhD degree in Power and Control from the University of Durham, England, in 1997.

Dr. Chen worked as a lecturer and then a senior lecturer in De Montfort University, Leicester, England. He has been a full professor in the Department of Energy Technology, Aalborg University, Denmark, since 2002. He is the leader of Wind Power System Research program at the Department of Energy Technology, Aalborg University. His main research interests are wind power, power electronics, power systems, and multi-energy systems.

In these areas, he has led and participated in many international and national research projects, has supervised many PhDs, postdoctoral researchers, visiting scholars, and visiting PhDs, and has more than 1000 technical publications. He is a panel member or review expert for many international funding organizations. Dr. Chen serves as a member of editorial boards for many international journals, including Associate Editor of the *IEEE Transactions on Power Electronics*, Deputy Editor of *IET Renewable Power Generation* (Wind Turbine Technology and Control), and Editor-in-Chief for the MDPI *Wind*.

Dr. Chen is a Fellow of IEEE, a Fellow of the Institution of Engineering and Technology (IET, London, UK), a Chartered Engineer in the United Kingdom, and a member of the Danish Academy of Technical Sciences.

Preface

With the rapid development of high-power semiconductor devices, power converters have been widely used in electric power conversion systems, converting electric power with high efficiency and economic benefit. The modular multilevel converter (MMC) is considered as one of the most promising converters for medium-/high-voltage and high-power applications because of its superior advantages, such as excellent output power quality, high efficiency, modularity, and scalability.

As increased MMCs are put into practical application, the concerns in terms of reliability and fault protection emerge to front stage. The semiconductor devices and capacitor are two most fragile components in the submodule of the MMC whose failure brings troubles to reliable operation of the MMC. And the MMC is usually required to have an uninterruptable operation ability in case of submodule malfunction. In addition, the AC-side grid fault and DC-side fault also pose challenges to the MMC system.

First, this book provides a brief review of the MMC basic principle and its control method in Chapters 1 and 2. Then, the insulated gate bipolar transistor fault detection methods and capacitor monitoring methods are respectively covered in Chapters 3 and 4. Chapter 5 offers fault-tolerant operation under submodule faults. Finally, Chapter 6 presents the control of MMCs under AC grid faults, and Chapter 7 explores the protection under DC short-circuit fault of the MMC system.

1

Modular Multilevel Converters

1.1 Introduction

Power converters have been widely used in electric power conversion systems that can convert electric power with high conversion efficiency and economic benefits. In the past few decades, several power converters have been developed and commercialized in the industrial community. They can be classified into current source converters (CSCs) and voltage source converters (VSCs).

The modular multilevel converter (MMC), as a kind of VSC, has been considered one of the most promising converters for medium/high-voltage and high-power applications, with the superiority such as excellent output power quality, high efficiency, modularity, and scalability [1–3]. Compared with traditional two-level and multilevel converters, the MMC has prominent advantages such as high efficiency and low power losses. What is more, high modularity enables the MMC to easily expand capacity. Recently, the MMC has become attractive for high-voltage direct-current (HVDC) transmission [4], renewable energy generation [5], electric railway supplies [6], micro power grid [7], etc.

This chapter deals with the fundamental principles of the MMC. The configuration of the MMC is presented in Section 1.2. Section 1.2 gives an introduction of the converter configuration and the submodule (SM) configuration. The operation principles of the SM and the converter are shown in Section 1.3. Section 1.4 demonstrates the modulation schemes, including phase-disposition (PD) pulse width modulation (PWM), phase-shifted (PS) PWM, and nearest level modulation (NLM). Afterward, mathematical models of the SM, the arm, and the MMC are introduced in Section 1.5. Then, Section 1.6 introduces the parameter design methods of power devices, capacitor, and arm inductor in the MMC. An overview of the MMC faults is given in Section 1.7.

1.2 MMC Configuration

1.2.1 Converter Configuration

A three-phase MMC topology is shown in Figure 1.1, which consists of three phase-legs, each composed of an upper arm and a lower arm. Each arm contains n identical SMs and an arm inductor L_s . The upper and lower arm currents are i_{ju} and i_{jl} , respectively, in phase j ($j = a, b, c$). The AC side of the MMC is equipped with the filter inductor L_f . The MMC links the DC side and the three-phase AC side. Electric power can flow from the DC side to the AC side or from the AC side to the DC side through changing the operation mode of the MMC. The number of SMs can affect the output voltage level and thus power quality. A multilevel voltage would be synthesized at the AC side of the MMC, and output harmonic contents would be reduced with the cascading of SMs [8].

1.2.2 Submodule Configuration

The SM unit is the fundamental component of the MMC. Figure 1.2 shows the typical half-bridge (HB) SM configuration, which is widely used in power

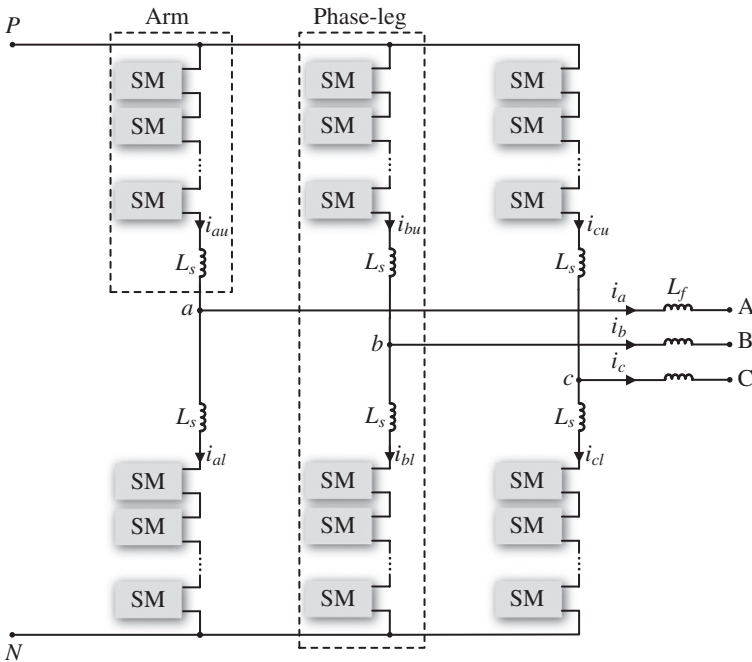
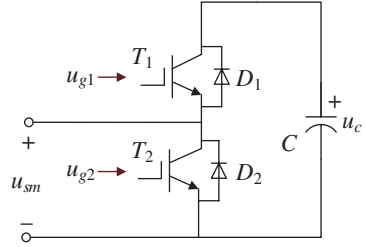


Figure 1.1 Three-phase MMC configuration.

Figure 1.2 Half-bridge SM.

applications. The HB SM consists of two switches/diodes T_1/D_1 and T_2/D_2 and a DC capacitor C . Through the switching of the power switches T_1 and T_2 , the HB SM can output two voltage levels, including the capacitor voltage u_c and 0 [8].

1.3 Operation Principles

1.3.1 Submodule Normal Operation

In the normal operation of the MMC, the operation state of the SM is controlled by the switching function S , which is defined as

$$S = \begin{cases} 1, & u_{g1} \text{ is high-level and } u_{g2} \text{ is low-level} \\ 0, & u_{g1} \text{ is low-level and } u_{g2} \text{ is high-level} \end{cases} \quad (1.1)$$

where u_{g1} and u_{g2} are the drive voltages of switches T_1 and T_2 , respectively, as shown in Figure 1.2. The switching modes of the HB SM are listed in Table 1.1.

- The T is turned on when the u_g is high-level
- The T is turned off when the u_g is low-level.

The relationship between the SM's output voltage u_{sm} and the SM's capacitor voltage u_c is

$$u_{sm} = S \cdot u_c \quad (1.2)$$

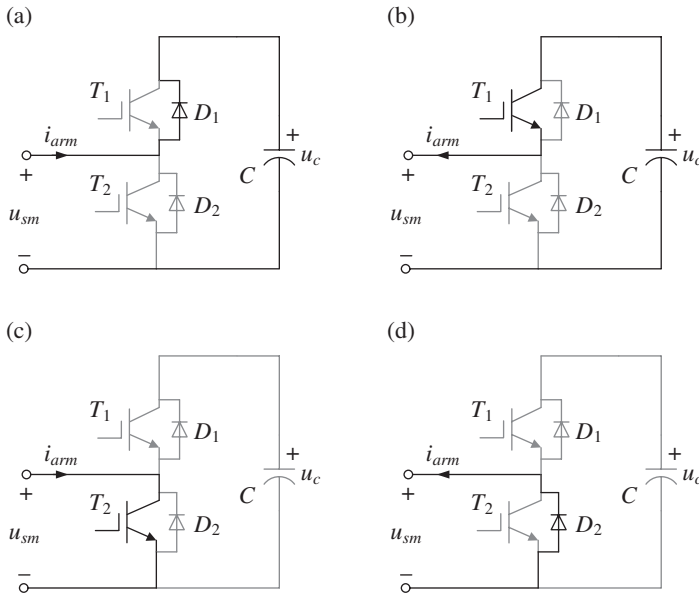
The normal operation of the HB SM has four operation modes, as shown in Table 1.2 and Figure 1.3, which are decided by the switching function S and the direction of the arm current i_{arm} , as follows:

Table 1.1 Switching modes of the HB SM.

| S | u_{g1} | u_{g2} | T_1 | T_2 |
|-----|------------|------------|-------|-------|
| 1 | High-level | Low-level | On | Off |
| 0 | Low-level | High-level | Off | On |

Table 1.2 Four normal operation modes of the HB SM.

| Mode | S | i_{arm} | Circuit state | SM state | T_1 | T_2 | u_{sm} | C | u_c |
|------|-----|-----------|---------------|----------|-------|-------|----------|------------|-----------|
| 1 | 1 | >0 | Inserted | On | On | Off | u_c | Charged | Increased |
| 2 | | <0 | Inserted | On | On | Off | u_c | Discharged | Reduced |
| 3 | 0 | >0 | Bypassed | Off | Off | On | 0 | Bypassed | Unchanged |
| 4 | | <0 | Bypassed | Off | Off | On | 0 | Bypassed | Unchanged |

**Figure 1.3** Four normal operation modes of the HB SM. (a) Mode 1 (normal operation). (b) Mode 2 (normal operation). (c) Mode 3 (normal operation). (d) Mode 4 (normal operation).

- **Mode 1 (normal operation):** When $S = 1$ and $i_{arm} > 0$, as shown in Figure 1.3a, the T_1 is turned on, the T_2 is turned off, the SM is inserted into the arm circuit, the SM state is on, and the SM output voltage u_{sm} is equal to the SM capacitor voltage u_c . In this case, the SM capacitor C is charged by i_{arm} , and the capacitor voltage u_c is increased.
- **Mode 2 (normal operation):** When $S = 1$ and $i_{arm} < 0$, as shown in Figure 1.3b, the T_1 is turned on, the T_2 is turned off, the SM is inserted into the arm circuit, the SM state is on, and the SM output voltage u_{sm} is equal to the SM capacitor

voltage u_c . In this case, the SM capacitor C is discharged by i_{arm} , and the capacitor voltage u_c is reduced.

- *Mode 3 (normal operation)*: When $S = 0$ and $i_{arm} > 0$, as shown in Figure 1.3c, the T_1 is turned off, the T_2 is turned on, the SM is bypassed from the arm circuit, the SM state is off, and the SM output voltage u_{sm} is equal to 0. In this case, the SM capacitor C is bypassed, and the capacitor voltage u_c is unchanged.
- *Mode 4 (normal operation)*: When $S = 0$ and $i_{arm} < 0$, as shown in Figure 1.3d, the T_1 is turned off, the T_2 is turned on, the SM is bypassed from the arm circuit, the SM state is off, and the SM output voltage u_{sm} is equal to 0. In this case, the SM capacitor C is bypassed, and the capacitor voltage u_c is unchanged.

1.3.2 Submodule Blocking Operation

In the blocking operation of the HB SM, the drive voltages u_{g1} and u_{g2} are both low-level and the switches T_1 and T_2 are both turned off, which has two operation modes and is decided by the arm current i_{arm} , as shown in Table 1.3 and Figure 1.4, as follows:

- *Mode 1 (blocking operation)*: When T_1 and T_2 are both turned off and $i_{arm} > 0$, as shown in Figure 1.4a, the SM is inserted into the arm circuit, the SM state is on, and the SM's output voltage u_{sm} is u_c . In this case, the capacitor C is charged by i_{arm} , and the capacitor voltage u_c is increased.

Table 1.3 Two blocking operation modes of the HB SM.

| Mode | i_{arm} | Circuit state | SM state | T_1 | T_2 | u_{sm} | C | u_c |
|------|-----------|---------------|----------|-------|-------|----------|----------|-----------|
| 1 | >0 | Inserted | On | Off | Off | u_c | Charged | Increased |
| 2 | <0 | Bypassed | Off | Off | Off | 0 | Bypassed | Unchanged |

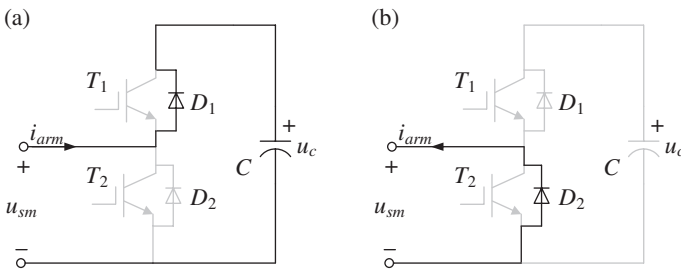


Figure 1.4 Two blocking operation modes of the HB SM. (a) Mode 1 (blocking operation). (b) Mode 2 (blocking operation).

- *Mode 2 (blocking operation)*: When T_1 and T_2 are both turned off and $i_{arm} < 0$, as shown in Figure 1.4b, the SM is bypassed from the arm circuit, the SM state is off, and the SM's output voltage u_{sm} is 0. In this case, the capacitor C is bypassed, and the capacitor voltage u_c is unchanged.

1.3.3 Converter Operation

The MMC generates the multilevel stepped waveform at its AC side by controlling the number of inserted SMs in the arm. To get an intuitive understanding of the operation principle of the MMC, Figure 1.5a shows an example of the upper arm of phase A, where four HB SMs (SM1–SM4) per arm are considered for the MMC. Here, all SMs' capacitor voltages are supposed to be the same as u_c , and the output voltages of the SM1–SM4 are u_{sm_au1} , u_{sm_au2} , u_{sm_au3} , and u_{sm_au4} , respectively. The waveform of the upper arm voltage u_{au} in phase A in one fundamental period is shown in Figure 1.5b, which is the sum of all SMs' output voltages u_{sm_au1} , u_{sm_au2} , u_{sm_au3} , and u_{sm_au4} in the upper arm of phase A. The switching functions of the SM1–SM4 and the corresponding output voltages of the SM1–SM4 are shown in Table 1.4, where the switching functions of

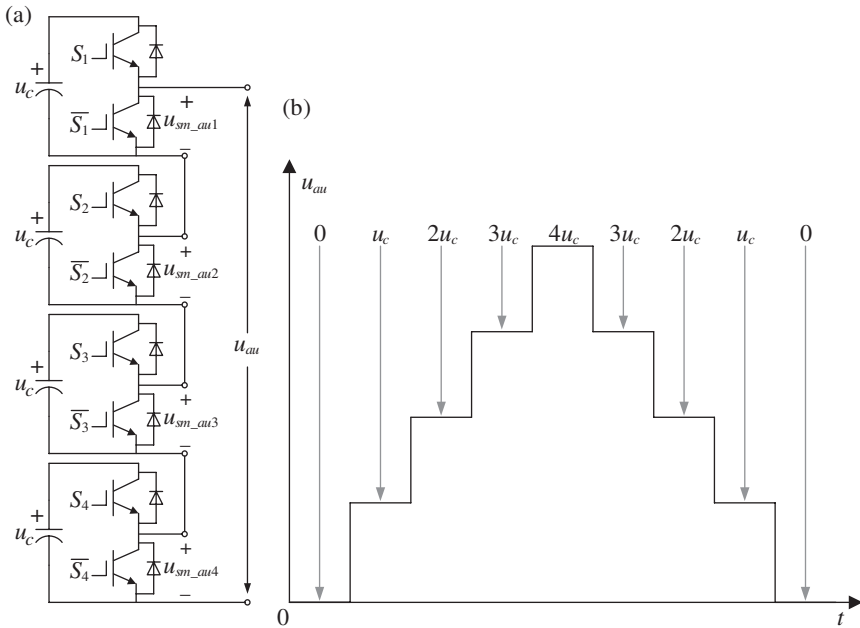


Figure 1.5 Operation principle of the MMC. (a) Upper arm of phase A. (b) Upper arm voltage of phase A.

Table 1.4 Switching functions and output voltages of SMs.

| n_{on} | S_{au1} | S_{au2} | S_{au3} | S_{au4} | u_{sm_au1} | u_{sm_au2} | u_{sm_au3} | u_{sm_au4} | u_{au} |
|----------|-----------|-----------|-----------|-----------|---------------|---------------|---------------|---------------|----------|
| 0 | 0 | 0 | 0 | 0 | 0 | 0 | 0 | 0 | 0 |
| | 1 | 0 | 0 | 0 | u_c | 0 | 0 | 0 | |
| | 0 | 1 | 0 | 0 | 0 | u_c | 0 | 0 | |
| | 0 | 0 | 1 | 0 | 0 | 0 | u_c | 0 | |
| | 0 | 0 | 0 | 1 | 0 | 0 | 0 | u_c | |
| 1 | 1 | 1 | 0 | 0 | u_c | u_c | 0 | 0 | u_c |
| | 1 | 0 | 1 | 0 | u_c | 0 | u_c | 0 | |
| | 1 | 0 | 0 | 1 | u_c | 0 | 0 | u_c | |
| | 0 | 1 | 1 | 0 | 0 | u_c | u_c | 0 | |
| | 0 | 1 | 0 | 1 | 0 | u_c | 0 | u_c | |
| 2 | 1 | 0 | 0 | 1 | u_c | 0 | 0 | u_c | $2u_c$ |
| | 0 | 1 | 1 | 0 | 0 | u_c | u_c | 0 | |
| | 0 | 1 | 0 | 1 | 0 | u_c | 0 | u_c | |
| | 0 | 0 | 1 | 1 | 0 | 0 | u_c | u_c | |
| | 1 | 1 | 1 | 0 | u_c | u_c | u_c | 0 | |
| 3 | 1 | 1 | 0 | 1 | u_c | u_c | 0 | u_c | $3u_c$ |
| | 1 | 0 | 1 | 1 | u_c | 0 | u_c | u_c | |
| | 0 | 1 | 1 | 1 | 0 | u_c | u_c | u_c | |
| 4 | 1 | 1 | 1 | 1 | u_c | u_c | u_c | u_c | $4u_c$ |

SM1–SM4 are S_{au1} , S_{au2} , S_{au3} , and S_{au4} , respectively. The arm voltage u_{au} has five different levels including 0, u_c , $2u_c$, $3u_c$, and $4u_c$, which is expressed as

$$u_{au} = \sum_{i=1}^4 u_{sm_au i} = \sum_{i=1}^4 (S_{au i} \cdot u_c) = n_{on} \cdot u_c \quad (1.3)$$

with

$$n_{on} = \sum_{i=1}^4 S_{au i} \quad (1.4)$$

where n_{on} is the number of inserted SMs in the arm of the MMC. The arm voltage u_{au} depends on different switching combinations corresponding to the SMs in the arm, as shown in Figure 1.5 and Table 1.4.

- *Fifth level* ($u_{au} = 4u_c$): The highest arm voltage $4u_c$ is generated when all four switching functions S_{au1} , S_{au2} , S_{au3} , and S_{au4} corresponding to the SM1–SM4 are all switched to 1.

- *Forth level* ($u_{au} = 3u_c$): The arm voltage $3u_c$ is generated when three out of four switching functions S_{au1} , S_{au2} , S_{au3} , and S_{au4} corresponding to the SM1–SM4 are switched to 1.
- *Third level* ($u_{au} = 2u_c$): The arm voltage $2u_c$ is generated when two out of four switching functions S_{au1} , S_{au2} , S_{au3} , and S_{au4} corresponding to the SM1–SM4 are switched to 1.
- *Second level* ($u_{au} = u_c$): The arm voltage u_c is generated when one out of four switching functions S_{au1} , S_{au2} , S_{au3} , and S_{au4} corresponding to the SM1–SM4 is switched to 1.
- *First level* ($u_{au} = 0$): The lowest arm voltage 0 is generated when all four switching functions S_{au1} , S_{au2} , S_{au3} , and S_{au4} corresponding to the SM1–SM4 are all switched to 0.

1.4 Modulation Scheme

Modulation is a technique that produces the desired voltage in the arm or at the AC side of the MMC by controlling the drive voltage of switching devices in the MMC. It affects not only the MMC's external performance, such as AC-side voltage harmonics and AC-side current harmonics, but also the internal characteristics, such as capacitor voltage fluctuation, distribution of energy, and power losses distribution among SMs [9]. Currently, there are three modulation schemes commonly used in the MMC, which are PD-PWM, PS-PWM, and NLM, as shown in Table 1.5. Based on the modulation and the reference y for the arm of the MMC, the number n_{on} of SMs to be inserted into the arm of the MMC can be decided, as shown in Figure 1.6.

Table 1.5 Three modulation schemes [9–16].

| Modulation scheme | Characteristics |
|-------------------|--|
| PD-PWM | <ul style="list-style-type: none"> • High switching frequency modulation • Unevenly distributed pulses • Suitable for MMCs with not so many SMs per arm |
| PS-PWM | <ul style="list-style-type: none"> • High switching frequency modulation • Evenly distributed pulses • Suitable for MMCs with not so many SMs per arm |
| NLM | <ul style="list-style-type: none"> • Low switching frequency modulation • Easy for implementation • Suitable for MMCs with large number of SMs per arm |

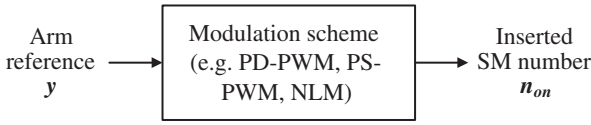


Figure 1.6 Modulation for MMCs.

1.4.1 Phase-Disposition PWM

The PD-PWM is typically suitable for the MMC with not so many SMs per arm [9–11]. For the MMC with n SM per arm, it is realized by applying n number of identical triangular carriers W_1 – W_n stacked evenly in the vertical direction between -1 and 1 . Through the comparison between the carriers and the reference signal y , the PD-PWM can be produced.

Figure 1.7 illustrates the implementation principle of the PD-PWM ($n = 4$) for the MMC with n SMs per arm. The n carriers W_1 – W_n are at the same phase angle. The carrier frequency is f_s . The height Δh of each carrier is equal to $2/n$.

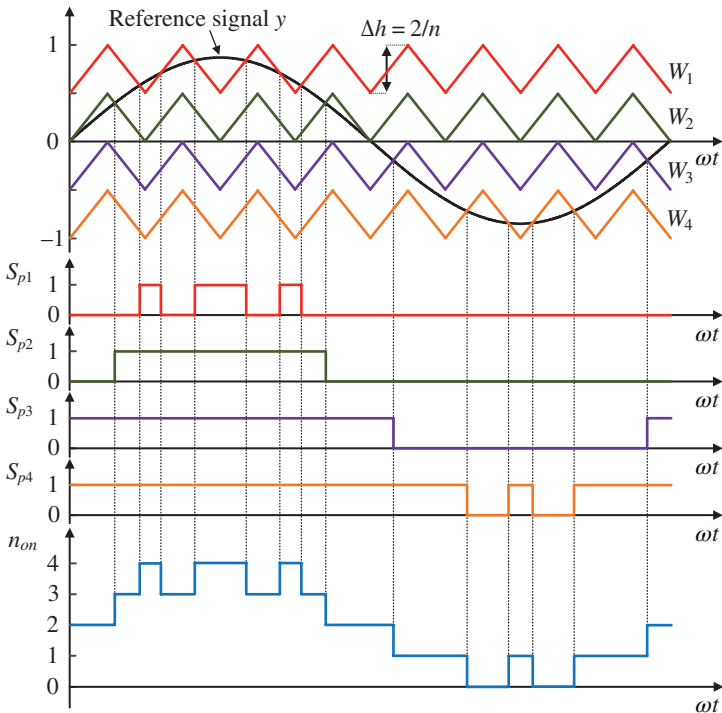


Figure 1.7 Implementation principle of PD-PWM for MMCs.

The reference signal y is compared with the carriers W_1-W_n to generate the pulses $S_{p1}-S_{pn}$, respectively, as follows:

- The S_{pi} is 1 if the reference y is higher than the carrier W_i ($i = 1, 2, \dots, n$)
- The S_{pi} is 0 if the reference is lower than the carrier W_i ($i = 1, 2, \dots, n$)

The total number n_{on} of SMs to be inserted into each arm at each instant can be expressed as the sum of $S_{p1}-S_{pn}$, as

$$n_{on} = \sum_{i=1}^n S_{pi} \quad (1.5)$$

Figure 1.7 shows that the PD-PWM results in an unevenly distributed switching frequency among $S_{p1}-S_{pn}$. The value of n_{on} varies in the range of $0-n$ in one fundamental period, which achieves the multilevel synthesized waveform. In addition, it is apparent that the switching actions of $S_{p1}-S_{pn}$ are affected by the amplitude of the reference signal y .

The typical characteristics of the PD-PWM are summarized in Table 1.5.

1.4.2 Phase-Shifted PWM

The PS-PWM is suitable for the MMC with not so many SMs per arm [12, 13]. For the MMC with n SMs per arm, it is realized by applying n number of identical triangular carriers W_1-W_n stacked evenly in horizontal direction. The carrier is between -1 and 1 . Through the comparison between the carriers W_1-W_n and the reference signal y , the PS-PWM can be achieved.

Figure 1.8 illustrates the implementation principle of PS-PWM ($n = 4$) for the MMC with n SMs per arm. The carriers W_1-W_n are all with the same carrier frequency f_s . The phase angle between two adjacent carriers of W_1-W_n is denoted as $\Delta\theta$. Generally, the $\Delta\theta$ is

$$\Delta\theta = 2\pi / n \quad (1.6)$$

The reference signal y is compared with the carriers W_1-W_n to generate the pulses $S_{p1}-S_{pn}$, as follows:

- The S_{pi} is 1 if the reference y is more than the carrier W_i ($i = 1, 2, \dots, n$)
- The S_{pi} is 0 if the reference is less than the carrier W_i ($i = 1, 2, \dots, n$)

The total number n_{on} of the SMs to be inserted into each arm at each instant can be expressed as the sum of $S_{p1}-S_{pn}$, as

$$n_{on} = \sum_{i=1}^n S_{pi} \quad (1.7)$$

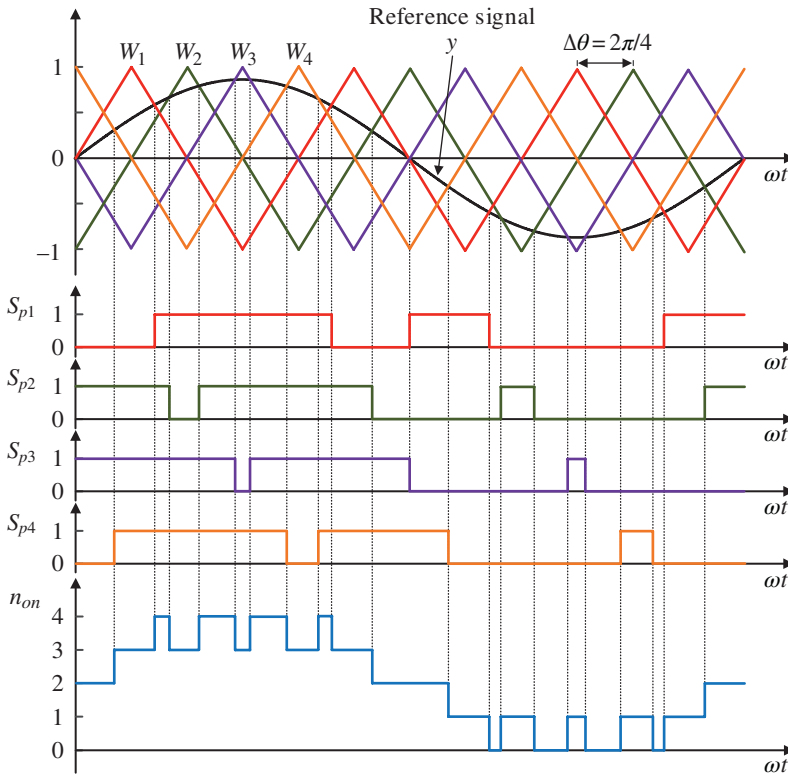


Figure 1.8 Implementation principle of PS-PWM for MMCs.

In Figure 1.8, the reference signal y is always modulated by all carriers W_1-W_n to generate the PWM pulses. The pulses and the switching frequency are distributed evenly among $S_{p1}-S_{pn}$. The value of n_{on} varies in the range of $0-n$ in one fundamental period, which achieves the multilevel synthesized waveform. In addition, the switching actions of $S_{p1}-S_{pn}$ remain constant regardless of the modulation index of the reference signal.

The typical characteristics of the PS-PWM are summarized in Table 1.5.

1.4.3 Nearest Level Modulation

The NLM is suitable for the MMC applications with large number of SMs, e.g. high voltage direct current (HVDC) transmission [9, 14–16]. The NLM uses the staircase waveform nearest to the desired reference signal. For the MMC with n SMs per arm, the NLM can be produced with the simple rounding function for the reference y .

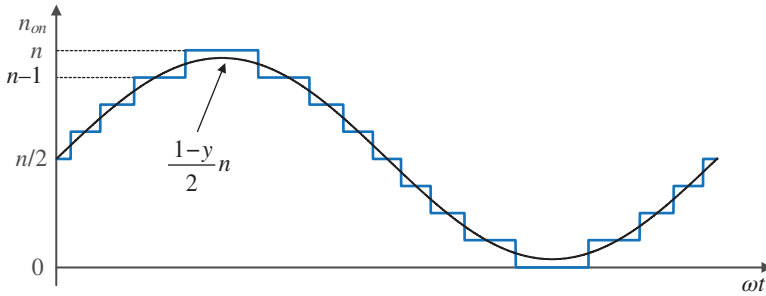


Figure 1.9 Implementation principle of NLM for MMCs.

Figure 1.9 illustrates the implementation principle of the NLM for the upper arm of the MMC ($n = 8$) with n SMs per arm. Based on the reference signal y for the phase unit, the total number n_{on} of SMs to be inserted into the upper arm at each instant can be obtained as

$$n_{on} = \text{round}\left(\frac{1-y}{2}n\right) \quad (1.8)$$

The NLM directly generates the number of inserted SMs in the arm to yield the multilevel waveforms. The waveform of n_{on} is a staircase with step height of 1. The value of n_{on} varies in the range of $0-n$. Therefore, the maximum level number of n_{on} is $n + 1$. The harmonic spectrum of the NLM is dependent on n . If n is small, the staircase number is small and the harmonics will be a little high. If n is large, the staircase number is large and the multilevel waveforms will be very close to the reference signal and have very little harmonics.

The typical characteristics of the NLM are summarized in Table 1.5.

1.5 Mathematical Model

1.5.1 Submodule Mathematical Model

Figure 1.10 shows the equivalent circuit diagram of the i -th SM in the upper arm of phase A. Figure 1.10a shows the equivalent circuit diagram of the SM when its switching function S_{aui} is 1, and Figure 1.10b shows the equivalent circuit diagram of the SM when its switching function S_{aui} is 0. According to the equivalent circuit diagrams, the switching-function based model and the reference-based model of the HB SM can be derived as discussed in the following sections.